



TITLE:

Suppression of insolation heating using paint admixed with silica spheres – An approach from infrared band electromagnetic scattering

AUTHOR(S):

Ohkawa, Eri; Mikada, Hitoshi; Goto, Tada-nori; Onishi, Kyosuke; Takekawa, Junichi; Taniguchi, Kiyoshi; Ashida, Yuzuru

CITATION:

Ohkawa, Eri ...[et al]. Suppression of insolation heating using paint admixed with silica spheres – An approach from infrared band electromagnetic scattering. Physics and Chemistry of the Earth, Parts A/B/C 2011, 36(16): 1412-1418

ISSUE DATE:

2011-01

URL:

<http://hdl.handle.net/2433/152172>

RIGHT:

© 2012 Elsevier B.V.; This is not the published version. Please cite only the published version.; この論文は出版社版ではありません。引用の際には出版社版をご確認ご利用ください。

Title: Suppression of Insolation Heating using Paint admixed with Silica Spheres –An approach from Infrared Band Electromagnetic Scattering–

Authors:

Eri Ohkawa

Kyoto University, Department of Civil and Earth Resources Engineering (Present at *Panasonic Electric Works Co., Ltd.*)

Hitoshi Mikada

Kyoto University, Department of Civil and Earth Resources Engineering (Corresponding Author*)

Tada-nori Goto

Kyoto University, Department of Civil and Earth Resources Engineering

Kyosuke Onishi

Kyoto University, Department of Civil and Earth Resources Engineering (Present at *Akita University*)

Junichi Takekawa

Kyoto University, Department of Civil and Earth Resources Engineering

Kiyoshi Taniguchi

Nittoc Construction Co., Ltd.

Yuzuru Ashida⁽³⁾

NPO EEFA

***Corresponding Author:**

Hitoshi Mikada

C1-1-112, Kyotodaigaku-Katsura, Nishikyo-ku

Kyoto 615-8540

Japan

Tel: +81-75-383-3196

Fax: +81-75-383-3198

E-mail: mikada@tansa.kumst.kyoto-u.ac.jp

ABSTRACT

The temperature of materials would be raised when the materials are exposed to the sunlight. Recently, it has been experimentally confirmed that such temperature rise may be restrained when coating the materials with paint admixed with fine silica spheres. Experimental consideration of this type of paint has been conducted, but how the paint controls the temperature rise has merely been clarified theoretically. The best diameter of the silica spheres to be admixed is not well understood, either. In this study, we hypothesized that the scattering of light would be attributed to restrain the temperature rise and tried to estimate the optimum size of the silica spheres. We confirmed that our hypothesis would be justified. In the calculation of the scattering intensity, the diameter of spheres in conjunction with the wavelength of incident lights would be the predominant parameter to the scattering effects. Our results might explain that our experimentally observed phenomenon is caused by the scattering of light, i.e., electromagnetic waves.

KEY WORDS: scattering, electromagnetic wave, silica spheres, Mie theory, heat radiation suppression

1. INTRODUCTION

It is well known that the insolation to buildings raises the temperature in rooms inside since part of the energy in the sunlight is thermally transferred to materials of outer wall of the buildings. As a consequence, the crisis of electric power supply could be caused by air conditioning in mid-summer. If room temperature is controlled without strong air conditioning, the consumption of energy, therefore, might be reduced and the heat island effects could be lowered. Recently, some experiments demonstrated that the room temperature could be kept low when the outer wall of buildings were coated with paint admixed with fine silica spheres whose diameters are in micron scale (Figure1). The mechanism of the temperature suppression with the silica-sphere-admixed paint has not been well investigated, although the interaction between silica spheres and the sunlight would be important in the observed phenomenon.

Studies about the interaction between spheres and the light have been done to focus on the diffraction of light by obstacles. Oster (1948) introduced light scattering theories in chemistry, Xu (1997) introduced Mie scattering for randomly distributed multiple spheres to estimate far field solution, Xu and Wang (1998) analyzed light scattering using amplitude scattering matrix, Miyazaki and Jimba (2000) studied light diffraction by bi-sphere, Miyazaki *et al.* (2003) solved light diffraction by double-layered microsphere lattice, Miyazaki *et al.* (2004) find characteristic spectral response by the double-layered microsphere lattice, etc. Since the interaction of silica spheres with the sunlight has not been attempted, it is necessary to focus on the above phenomenal experience to theoretically clarify what are the controlling factors. We could find coating compounds optimum to coated materials, once the mechanism of the interaction between silica spheres and the sunlight.

Fig.1

In this study, we aimed to find out the mechanism of the temperature suppression. We hypothesized that the electromagnetic waves in a certain frequency range were scattered to restrain the transmission of radiated energy in the insolation to insulated materials. For verifying the hypothesis, we used the Mie theory to calculate the intensity of scattered light by a set of packed spheres, since the diameter of spheres comparable to the incident sunlight wavelength are dealt with. As a result, we found that the amplitude of scattered light depends on the wavelength of incident light and the sizes of spheres. We conclude that these two parameters are the most important factors for achieving our objectives.

2. SCATTERING OF LIGHT

When an electromagnetic wave is incident upon a material at a frequency near the eigenfrequencies of atoms, molecules or bindings of the material, the atoms or molecules resonate or oscillate intensely, resulting in the temperature rise of the material. Since the light is an electromagnetic wave, the scattering of the sunlight would be attributed to the restraint phenomenon of the temperature rise. Therefore, we focus on the temperature rise that could be controlled if the electromagnetic waves around the eigenfrequencies are attenuated. Considering these possible interactions, we hypothesize that the intensity of light incident upon the paint layer is weakened due to the scattering of light by silica spheres near the eigenfrequencies of the atomic or molecule vibrations when propagating through the layer. Since the material used to cover building is not fixed, we assumed that the temperature rise of metal is controlled by the electromagnetic radiation of the wavelength in the near infrared band.

For the verification of the hypothesis, we first examine the relation between an incident wave and the scattered wave for a varying combination of wavelength of the incident wave and the diameter of a silica sphere. We used the Mie theory (Born and Wolf, 1999) to estimate the scattered wave caused by each sphere in the paint. In the Mie theory,

it has been theoretically solved for the diffraction of a plane monochromatic wave incident upon a uniform sphere in a homogeneous medium. Then, we extend the theory to the situation in which multiple spheres of the same physical property are aligned or in a space of homogeneous medium. However, in this study, the interaction of scattered wavefield with the other spheres in the plane of wavefront was not considered for simplicity.

3. SCATTERING BY SINGLE MICROSPHERE

First, the scattering of an electromagnetic wave by a single microsphere is examined by using the Mie theory. Using the Mie theory, theoretical solution to the scattered light by the single microsphere has been given in the spherical coordinates (r, θ, ϕ) whose origin is set at the center of a spherical scatterer (Figure 2) as follows (Born and Wolf, 1999).

$$\begin{aligned} E_r^{(S)} &= \frac{1}{(k^{(I)})^2} \cdot \frac{\cos \phi}{r^2} \sum_{l=1}^{\infty} l(l+1) {}^e B_l \zeta_l^{(I)}(k^{(I)}r) P_l^{(I)}(\cos \theta) \\ E_{\theta}^{(S)} &= \frac{1}{k^{(I)}} \cdot \frac{\cos \phi}{r} \sum_{l=1}^{\infty} \left\{ {}^e B_l \zeta_l^{(I)'}(k^{(I)}r) P_l^{(I)'}(\cos \theta) \sin \theta - i^m B_l \zeta_l^{(I)}(k^{(I)}r) P_l^{(I)}(\cos \theta) \frac{1}{\sin \theta} \right\} \\ E_{\phi}^{(S)} &= \frac{1}{k^{(I)}} \cdot \frac{\sin \phi}{r} \sum_{l=1}^{\infty} \left\{ {}^e B_l \zeta_l^{(I)'}(k^{(I)}r) P_l^{(I)}(\cos \theta) \frac{1}{\sin \theta} - i^m B_l \zeta_l^{(I)}(k^{(I)}r) P_l^{(I)'}(\cos \theta) \sin \theta \right\} \end{aligned} \quad (1)$$

Fig.2

where parameters denoted by E , k , B and functions ζ and P are for the electrical field, wavenumber, coefficient, the Riccati's Bessel function of the third kind and the associated Legendre function, respectively. The dash denotes the differentiation of the function by the parameter. The subscripts r, θ, ϕ and l are respectively for the spherical coordinates and for the order of the expansion in the solutions. The right-shoulder superscripts (S) and (I) , and the left-shoulder superscripts e and m are for the scattered, properties of the surrounding material, coefficient that appears in TE and TM modes in electromagnetic wave propagation, respectively. The right-shoulder superscripts (II) that did not appear in Eq. (1) is for the material filling the sphere. The functions ζ and P superscripted by (1) are expressed as follows.

$$\begin{aligned} \zeta_l^{(1)}(\rho) &= \sqrt{\frac{\pi \rho}{2}} H_{l+\frac{1}{2}}^{(1)}(\rho) \\ P_l^{(1)}(\cos \theta) &= \sin \theta \cdot P_l'(\cos \theta) \end{aligned}$$

where H_l and P_l are the l -th order Hankel function of the first kind and the Legendre function, respectively. The coefficients in Eq. (1) for both TE and TM modes can be expressed as follows.

$$\begin{aligned} {}^e B_l &= i^{l+1} \frac{2l+1}{l(l+1)} \cdot \frac{\hat{n} \psi_l'(q) \psi_l(\hat{n}q) - \psi_l(q) \psi_l'(\hat{n}q)}{\hat{n} \zeta_l^{(1)'}(q) \psi_l(\hat{n}q) - \zeta_l^{(1)}(q) \psi_l'(\hat{n}q)} \\ {}^m B_l &= i^{l+1} \frac{2l+1}{l(l+1)} \cdot \frac{\hat{n} \psi_l(q) \psi_l'(\hat{n}q) - \psi_l'(q) \psi_l(\hat{n}q)}{\hat{n} \zeta_l^{(1)}(q) \psi_l'(\hat{n}q) - \zeta_l^{(1)'}(q) \psi_l(\hat{n}q)} \end{aligned} \quad (2)$$

The function ψ_l is the l -th order modified spherical Bessel function of the first kind. Parameters q and \hat{n} are the dimensionless scale factor and the relative complex refractive index of the surrounding material against the sphere, respectively. They are expressed as follows.

$$\begin{aligned} q &= 2\pi \frac{a}{\lambda^{(I)}} \\ \hat{n} &= \frac{\hat{n}^{(II)}}{\hat{n}^{(I)}} \end{aligned}$$

where a , \hat{n} and λ are the radius of the sphere, the refractive index and the wavelength of the incident electromagnetic plane wave, respectively.

In this study, we suppose that the surrounding homogeneous material (I) and the sphere (II) are the air and silica, respectively. Therefore, we assume that the specific inductive capacities and the electrical conductivities of the materials (I) and (II) are: $\epsilon^{(I)} = 1.0$, $\epsilon^{(II)} = 1.95$, $\sigma^{(I)} \approx 0(S/m)$, and $\sigma^{(II)} = 1.0 \times 10^{-15}(S/m)$ in the following calculation. The speed of light in the vacuum is also assumed as $c = 3.0 \times 10^8(m/sec)$. The direction of the incident plane wave and the electrical field vector are assumed to be in the positive direction along the z-axis and along the x axis, respectively, in the Cartesian coordinates. The amplitude of the electrical field was set to the unity. We used a simulation package (Press, et al., 1992) for the evaluation of the special functions in eqs. (1) and (2). In the numerical calculations, we ignored the influence of scattering sources higher than 20-th order and truncated the summation in eq. (1).

Fig.3

We first confirmed that our simulations would give the adequate estimates to the scattering intensity as many of the other researchers have shown in the thick literature. Figure 3 depicts the scattering intensity when the dimensionless scale factor is set to 0.6π for a distance of $0.1 \mu m$. Figure 4 shows the difference of the scattering intensity projected on the z-x plane as a function of scattering angle for the two values of the dimensionless scale factor. Since the scatterer works as a secondary wave source, these intensity distributions could be regarded as radiation patterns from the scatterer for a plane wave incidence. In both cases, the radius of the scatterer was set as $0.5 \mu m$. Our numerical results clearly indicate that longer the wavelength becomes, weaker the scattering intensity and the scattering-angle dependency become. This means that the scattering approaches to that of Rayleigh scattering when the wavelength becomes longer. These results support what has been found by the other authors (Blumer, 1925; LaMer, et al., 1946a, 1946b; Oster, 1948). We therefore concluded that our numerical simulation functions with an accuracy enough to deal with the following scattering properties by multispheres even in the truncation of infinite series to the 20-th order.

Fig.4

4. SCATTERING BY MULTISPHERES

Fig.5

On the basis of the scattering by a single sphere, we next examine the scattering by multiple spheres since many spheres are contained in the paint. When the number of spheres increases, scattered waves could be scattered by the other scatterers. However, we used the Born approximation (Figure 5) to avoid the complexity caused by multiple scattering in our estimation. The Cartesian coordinates are set to an incident plane wave just like in the case of a single sphere. For estimating the effects of multiple spheres, we first examined the effect of a single scattering layer in which many scatterers of the same radius are aligned in a gridded way (Figure 6) to form a single layer parallel to the wavefront or perpendicular to the direction of wave propagation direction. Since the electromagnetic waves are influenced by each scatterer for an area larger than the size of the scatterer, we assumed scattering radius of the first Fresnel zone for a plane that is distant at twice the radius of the scatterer in the direction of z-axis. In other words, the spheres form a reflector plane perpendicular to the incident electromagnetic waves as shown in Figure 6. Our formulation is not exact as briefly described in Born and Wolf (1999), but is equivalent to the assumption that the following relationship holds for the scattering.

Fig.6

$$\begin{aligned} E^{(S)} &= p \iiint_V E^{(I)} G(\vec{r}, \vec{r}') d^3 r' \\ &= p \int_z \left(\iint_{x,y} E^{(I)} G(z, \vec{r}') dx dy \right) dz \\ &= p \int_z E_{xy}^{(S)}(z) dz \end{aligned} \quad (3)$$

In eq.(3), $E^{(I)}$ and $E^{(S)}$ denote the incident and the scattered electromagnetic waves, respectively. The function $E_{xy}^{(S)}$ indicates the wave scattered by a plane of spherical scatterers as in Figure 6. The function $G(\vec{r}, \vec{r}')$ is in general the free-space Green's function but is replaced by the equation (1). The value p is a constant.

Fig.7

In the present study, the radius of the sphere is assumed to be $0.5 \mu m$ using the peak grain size that was used for the experiments in Figure 1. The wavelength range is fixed from 0.75 to $2.5 \mu m$ for the near infrared light, and the size of the Fresnel zone is chosen as 6.5 times the radius of the sphere that is for the light of $2.5 \mu m$ at a distance of the diameter of sphere. Figure 7 depicts the total energy caused by a single layer of the scatter plane composed of 90000 spheres (300 each for x and y coordinates) for confirming energy conservation. E_i and E_s denote the incident and the forward scattered energies, respectively. For longer wavelength in the near infrared band, the transmitted energy is slightly higher than for the shorter wavelength because of the geometrical scattering that may become ascendent. We assumed that the energy not transmitted through the plane of scatterers would be either reflected back or absorbed to radiate back. Therefore the total reflected energy may be regarded as the fraction of the transmitted energy to the unity for every wavelength.

Our first assumption is that the temperature rise of metal is controlled by the electromagnetic radiation of the wavelength in the near infrared band. Therefore, in the following verification of our hypothesis, we concentrated on the wavelength band to the near infrared one. We also assumed that the spectrum of the insolation to the coated material could be expressed as in Figure 8 and that the thickness of each plane of scatterers were set to the diameter of the spheres and the total thickness of the coating was set to 100 μm . As shown in Figure 7, a single layer of scatterer has very low reflection coefficient but the stack of low-reflective layers could have high reflection coefficient due to multiple reflections even if the material filling the gap between each scatterer is vacant.

When a reflection coefficient is given as R for each layer of scatterers, the total reflection (R_N) and transmission (T_N) coefficients for the number of layers of N are given as follows (Claerbout, 1976).

$$\begin{aligned} T_N &= \frac{1 - R}{1 + (N - 1)R} \\ R_N &= \frac{NR}{1 + (N - 1)R} \end{aligned} \quad (4)$$

For the insolation of the wavelength in the infrared band, the total reflection coefficient as a function of the radius is shown in Figure 9. Finer becomes the sphere, higher becomes the reflection coefficient of the stack of the sphere layers, i.e., lower the transmission energy.

5. DISCUSSIONS

The objective of the present study is to clarify the mechanism that controls the temperature rise of the metal in the insolation by coating paint with fine silica spheres of micron scale. Also we wanted to know an effective size of the spheres. For this objective, we hypothesized that the scattering of light attributes to lower the temperature rise in the near infrared band that is near the characteristic frequency of the metallic bond. We then applied the Mie theory and solved the diffraction problem when a plane electromagnetic wave is incident to a silica sphere.

First we confirmed that the radiation pattern of scattered wave is a function of dimensionless scale factor q and r relative complex refractive index of the surrounding material against the sphere n . When either the dimensionless scale factor q becomes much greater than the unity or relative complex refractive index becomes much smaller than the unity, the entire scattered waves are intensified as described in Born and Wolf (1999). When the phenomenon becomes the Rayleigh scattering for the dimensionless scale factor that becomes much smaller than the unity, further simplification becomes possible (Born and Wolf, 1999). However, the present study deals with the scattering that cannot be simplified using the asymptotic solutions.

In the electromagnetic scattering, scattering cross section is larger than the physical size of a scatterer. Since we deal with the spherical scatterer, we define a scattering radius as a radius of the circular scattering cross section. It was confirmed that careful selection of scattering radius to be the size of the first Fresnel zone could give us a scattered plane wave field for a group of gridded scatterers in a plane. We also tried to simplify the calculations using the Born approximation using the exact solutions of mono-spherical scattering problem as a free-space Green's function. The number of spheres to constitute a scatterer plane is determined after confirming a plane scattered wavefield to be formed. Finally, the stack of the plane of scatterers is assumed to model the layer of paint. We think this approach must be revisited to see if our assumptions are adequate or not again since the regular-gridded arrangement of scatterers is not realistic nor the filling between scatterers is assumed to be the air.

Using a simple multiple reflection theory, our results demonstrate that smaller the sphere becomes, weaker is the transmitted energy through the stack of scatterer layers using a simple multiple reflection theory. However, we do not think that the reflection coefficients in the results (Figure 9) could explain almost the same temperature variation as the air temperature observed in the field. We think that the present study deals only with the initial and fundamental approximation but could explain the observed phenomenon for the practice of real painting using silica spheres (Fig.1). Although we ignored the multiple scattering effects in our numerical calculations, the results also indicates that the scattering of scattered waves may play an important role to fully explain the observed phenomenon as for the multiple reflections we included in the calculations. Although the infinite series was truncated in the present study up to the 20th order, the influence of disregarded higher-order terms would not be negligible for the dimensionless scale factors become much less than the unity. We think that systematic and experimental studies must be conducted to testify our numerical results.

The assumptions and the simplifications we made was: (i) absorption of near-infrared band lights would raise the temperature of the absorbing material, (ii) transmitted energy through the stack of scatterer layers would all be absorbed by the metal, (iii) the light was incident perpendicular to the surface of the stack of the scatterer layers, and (iv) electromagnetic field could represent the intensity of light, (5) the infinite series in eq.(1) could be truncated at the 20-th

Fig.8

Fig.9

order, etc. These assumptions need to be confirmed to assure the validity of the present calculations. Also, any fluorescence-like resonance scattering phenomena were ignored to constrain our discussions in the linear physical phenomena. Since the wavelength of lights we have dealt with in the present study is comparable to the size of spheres, resonance scattering could take place. The effects of resonance scattering should be checked to confirm the validity of our study. An assumption that the spherical scatterers are suspended in the air should be modified so that the scatterers are buried in the paint. Since the lights passing through the paint would be weakened absorbed by the paint material, the reflection and transmission coefficients would surely become different from the present results. The transmission coefficients, however, would be lowered than in the present study.

6. CONCLUSIONS

The present study tried to explain the phenomenon that the temperature rise of metal roof is lowered when the roof is coated by paint admixed with fine silica spheres. We also would like to find the effective size of the silica spheres based on a hypothesis that the scattering of light in the near infrared band attributes to the moderation effects on heating by the solar radiation.

The hypothesis was tested using the Mie theory. Due to the complexity in the theory, we tried to simplify the calculations using pseudo-Born approximation, truncation at finite order of the infinite series, reflection coefficients, etc. Our results demonstrate that the scattering effects must be one of causes to explain the observed moderation of the temperature rise in the insolation when the stack of layers of silica spheres exist. The transmission of the electromagnetic waves, whose wavelengths are in near infrared, i.e., the characteristic frequency of metallic bond, are weakened due to scattering. We also estimated the total reflection coefficients when the thickness of the scatterer layers is 100 μm becomes higher as the radius of each sphere approaches to shorter wavelength of the near infrared band.

We would like to conclude that the first approach to explain the phenomenon is successful but the further verification is necessary to overcome the imitations that may be caused by our simplification.

REFERENCES

- Blumer, H., 1925, Strahlungsdiagramme kleiner dielectrischer Kugeln, *Z. Phys.*, **32**, 119-134.
- Born, M., and Wolf, E., 1999, *Principles of optics*, 7th edition, Cambridge University Press, 952pp.
- Claerbout, J.F., 1976, *Fundamentals of Geophysical Data Processing*, McGraw-Hill, 274pp.
- Japan Solar Energy Society, 1985, *Handbook of Solar Energy Use*, Japan Solar Energy Society, 841pp.
- LaMer, V. K., and M. D. Barnes, 1946a, Monodispersed hydrophobic collidal dispersions and light scattering properties. I. Preparation and light scattering properties of monodispersed colloidal sulfur, *J. Col. Sci.*, **1**, 71-77.
- LaMer, V. K., and M. D. Barnes, 1946b, Monodispersed hydrophobic collidal dispersions and light scattering properties. II. Total scattering from transmittance as a basis for the calculation of particle size and concentration, *J. Col. Sci.*, **1**, 79-91.
- Miyazaki, H., and Jimba, Y., 2000, Ab initio tight-binding description of morphology-dependent resonance in a bisphere, *Phys. Rev. B*, **62**, 7976-7997, doi: 10.1103/PhysRevB.62.7976.
- Miyazaki, H., Miyazaki, H. T., Shinya, N., and Miyano, K., 2003, Enhanced light diffraction from a double-layer microsphere lattice, *Appl. Phys. Lett.*, **83**, 3662-3664, doi:10.1063/1.1623932.
- Miyazaki, H. T., Miyazaki, H., Jimba, Y., Kurokawa, Y., Shinya N., and Miyano K., 2004, Light diffraction from a bilayer lattice of microspheres enhanced by specular resonance, *J. Appl. Phys.*, **95**, 793-805, doi:10.1063/1.1636254.
- Oster, G., 1948, Applications of light scattering to chemistry, *Chem., Rev.*, **43**, 319-365.
- Press, W.H., S. A. Teukolsky, W. T. Vetterling and B. P. Flannery, 1992, *Numerical Recipes in FORTRAN 77*, second edition, Cambridge University Press, 933pp.
- Xu, Y. L., and Wang, R. T., 1998, Electromagnetic scattering by an aggregate of spheres: theoretical and experimental study of the amplitude scattering matrix, *Phys. Rev. E*, **58**, 3931-3948, doi:10.1103/PhysRevE.58.3931.
- Xu, Y. L., 1997, Electromagnetic scattering by an aggregate of spheres: far field, *Applied Optics*, **36** (36), 9496-9508.

Acknowledgement

The authors are indebted to the anonymous reviewers for the discussions and suggestions to the manuscript. Also to Ms. Madoka Mikada and Shiori Okamoto for their help to read data and draw figures. This paper was originally prepared as a master thesis of Eri Ohkawa. The authors are grateful to Japan Society for the Promotion of Science who supported this study in Grant-in-Aid for Scientific Research (C) #19560811 and to the Mitsubishi Foundation for Research Funding.

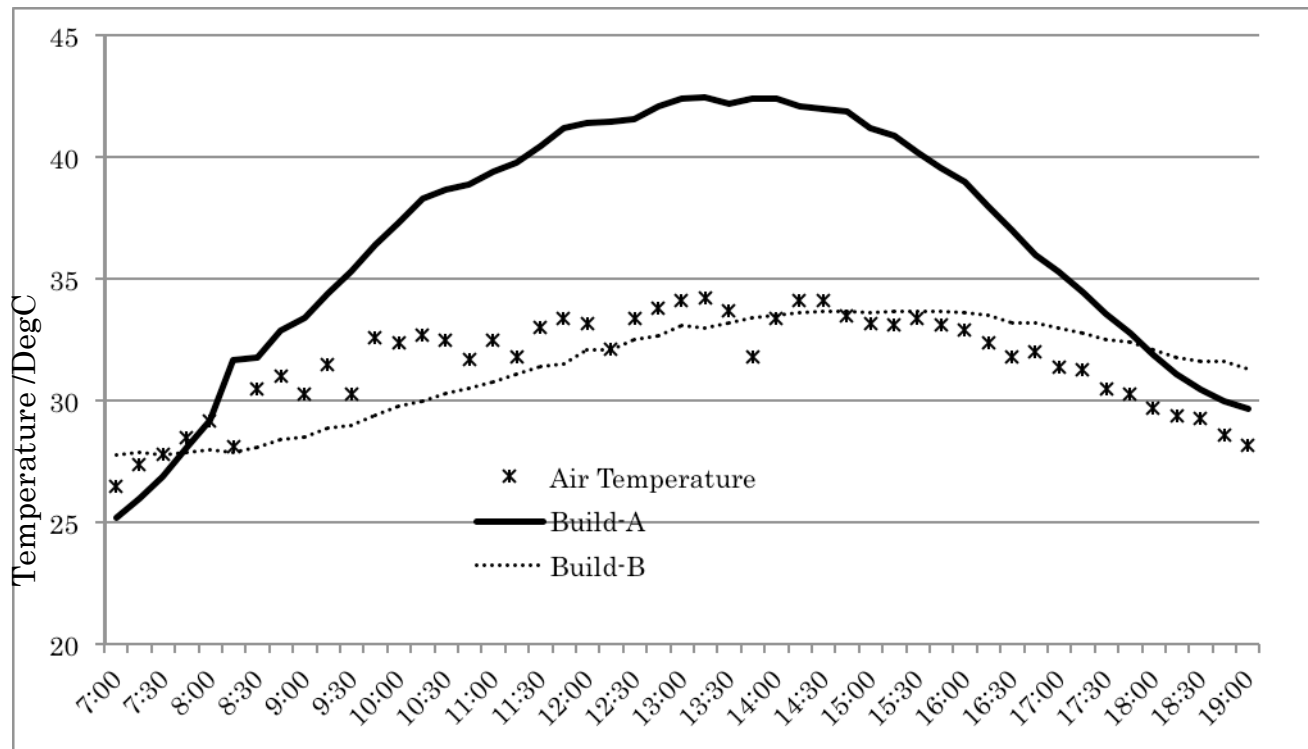


Figure 1(a)

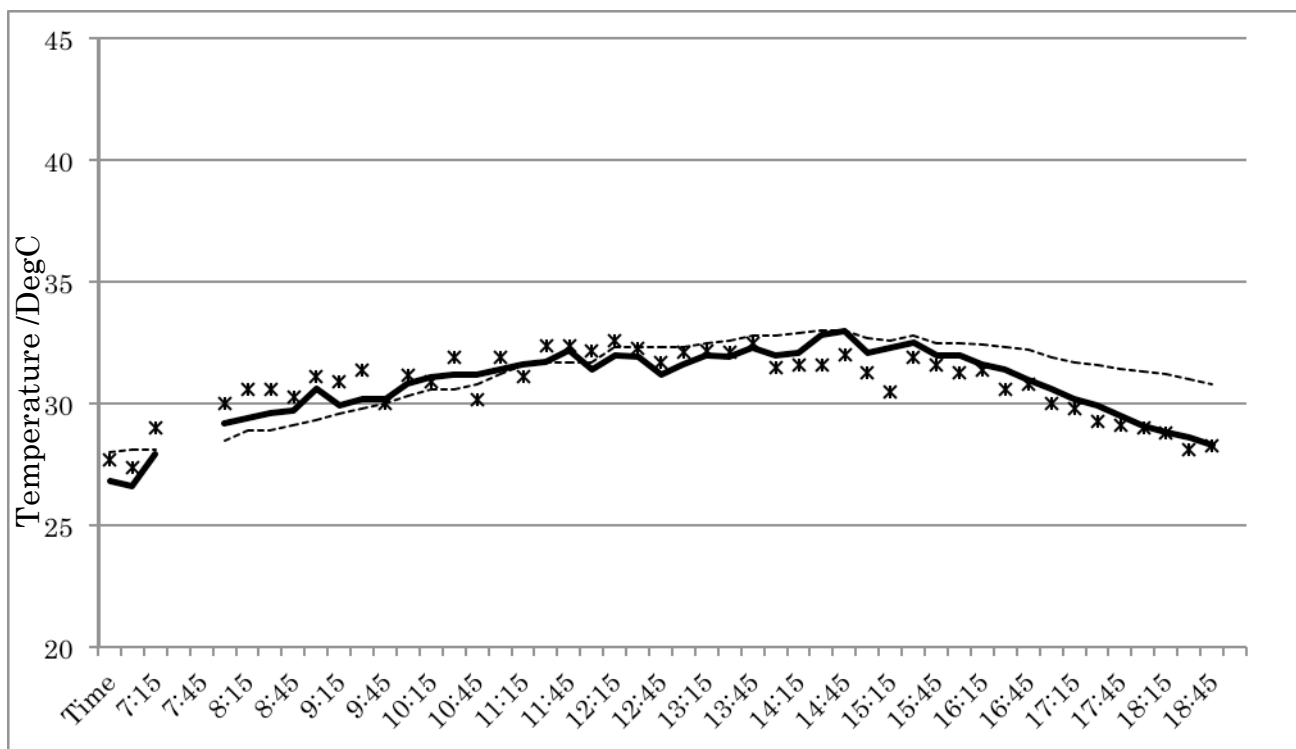


Figure 1(b)



Figure 1(c)



Figure 1(d)

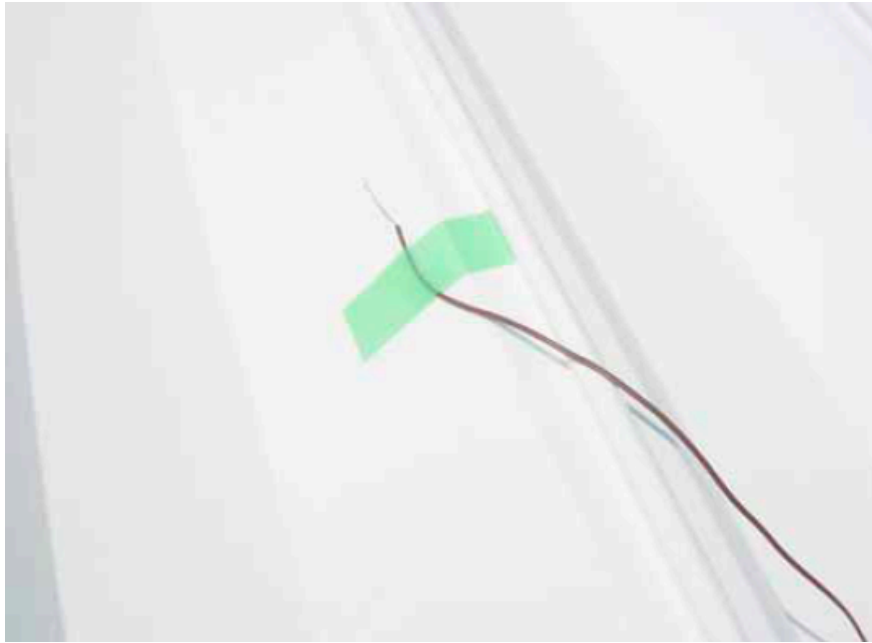


Figure 1(e)

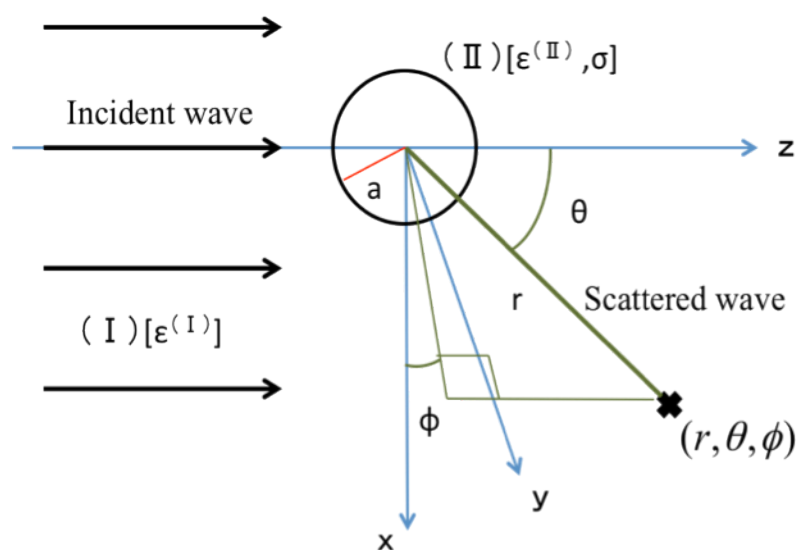


Figure 2

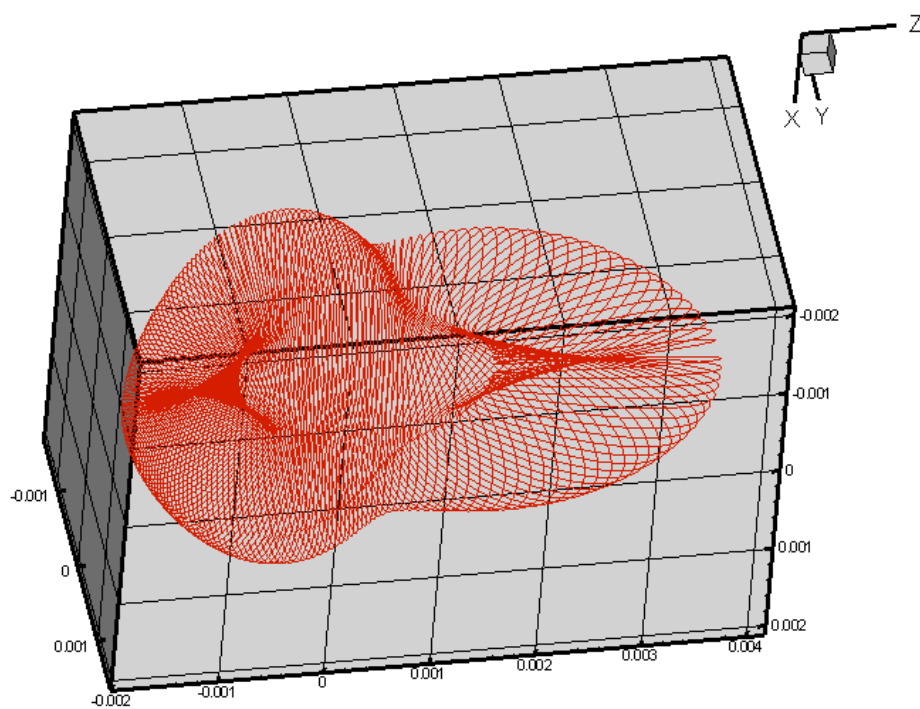


Figure 3

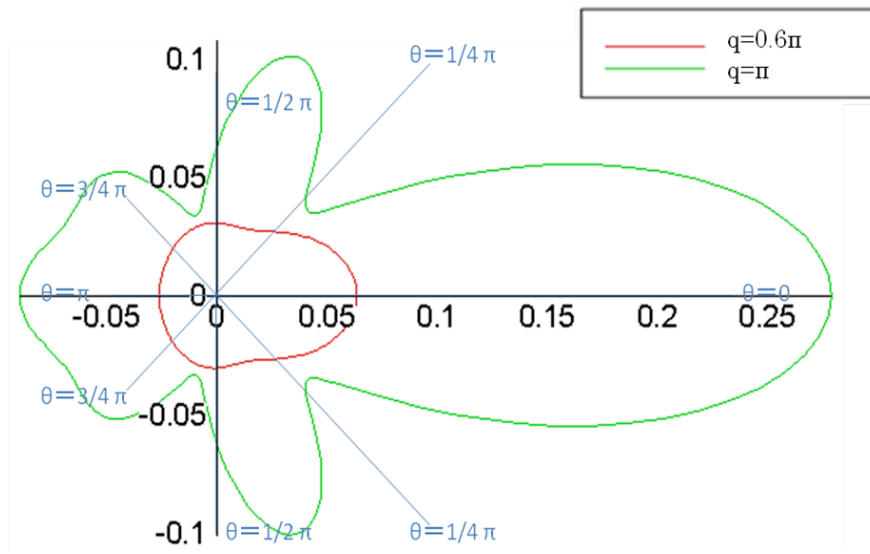


Figure 4

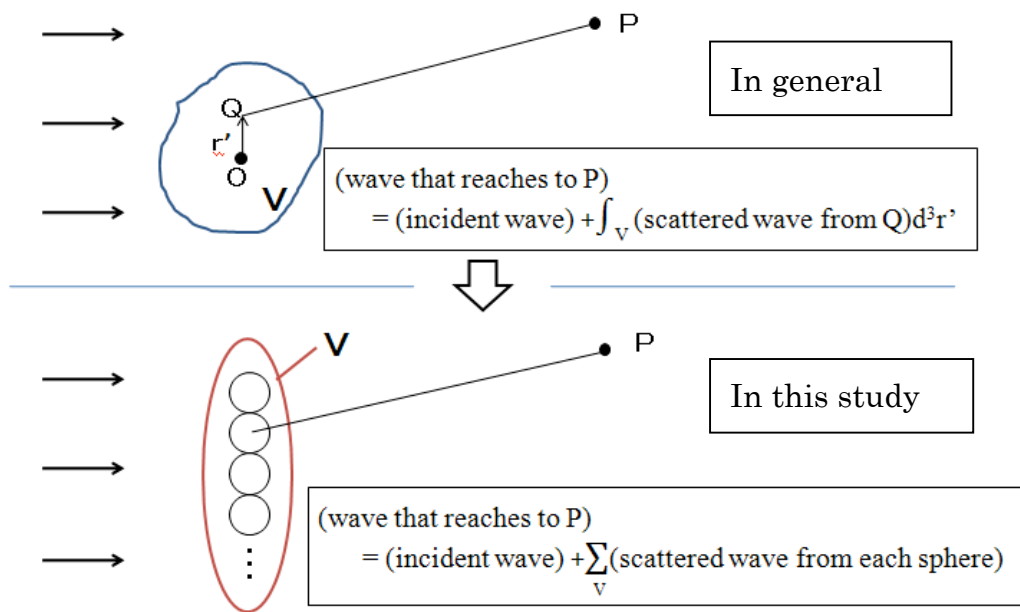


Figure 5

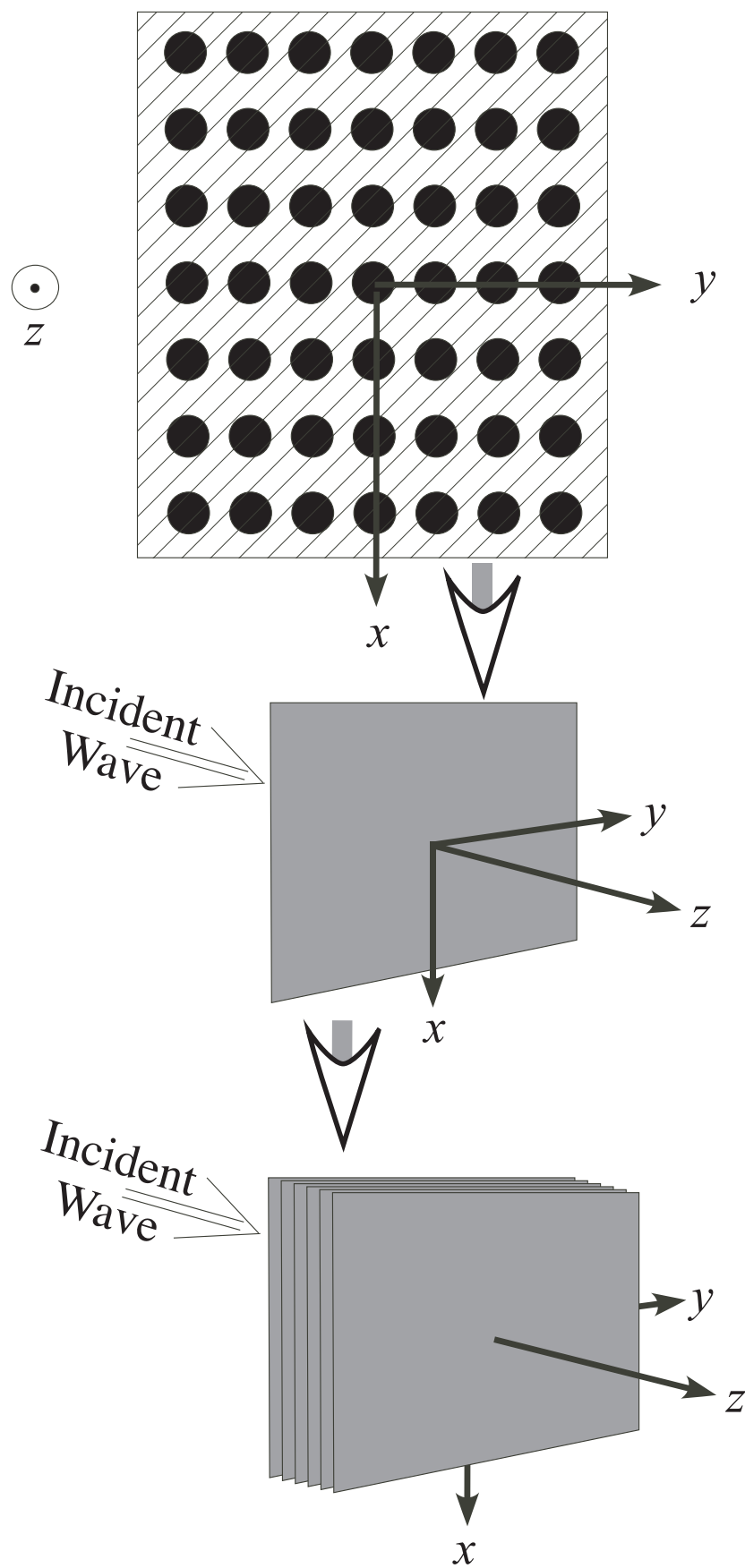


Figure 6

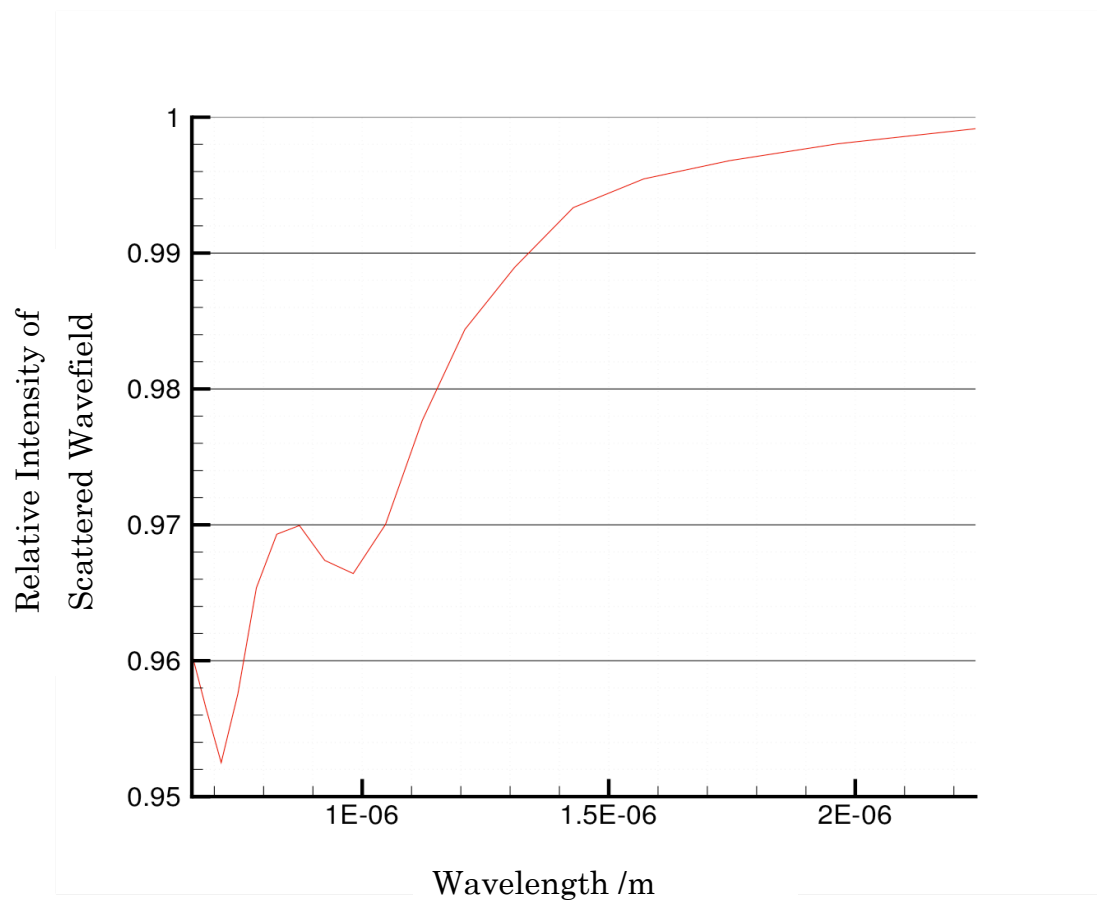


Figure 7

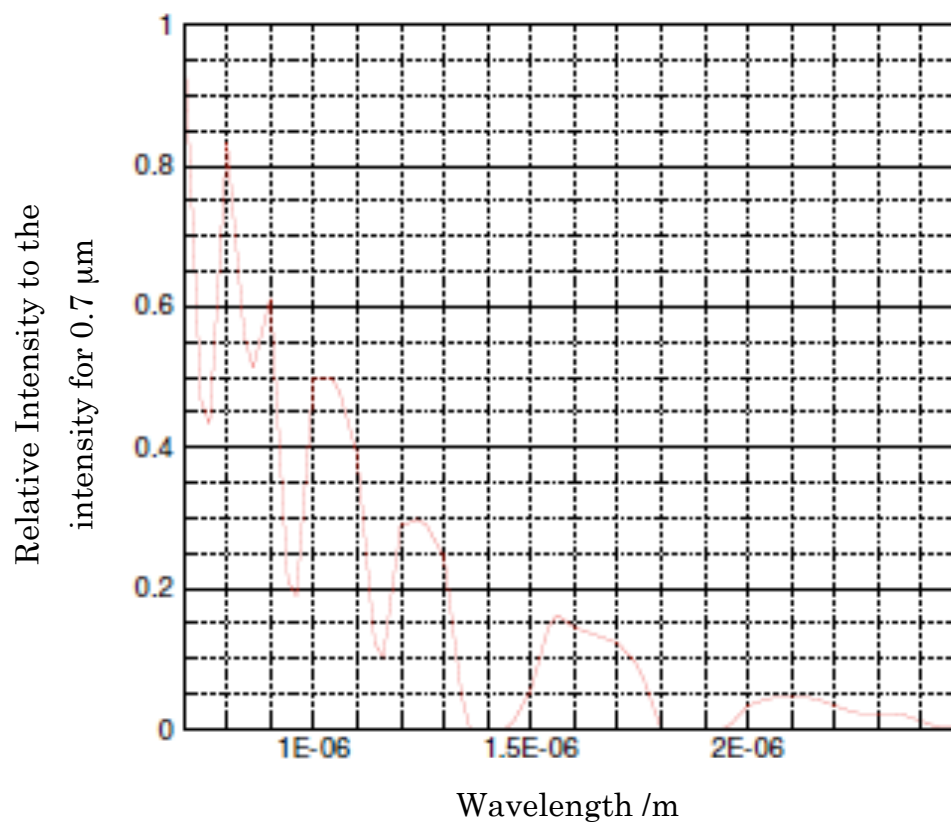


Figure 8

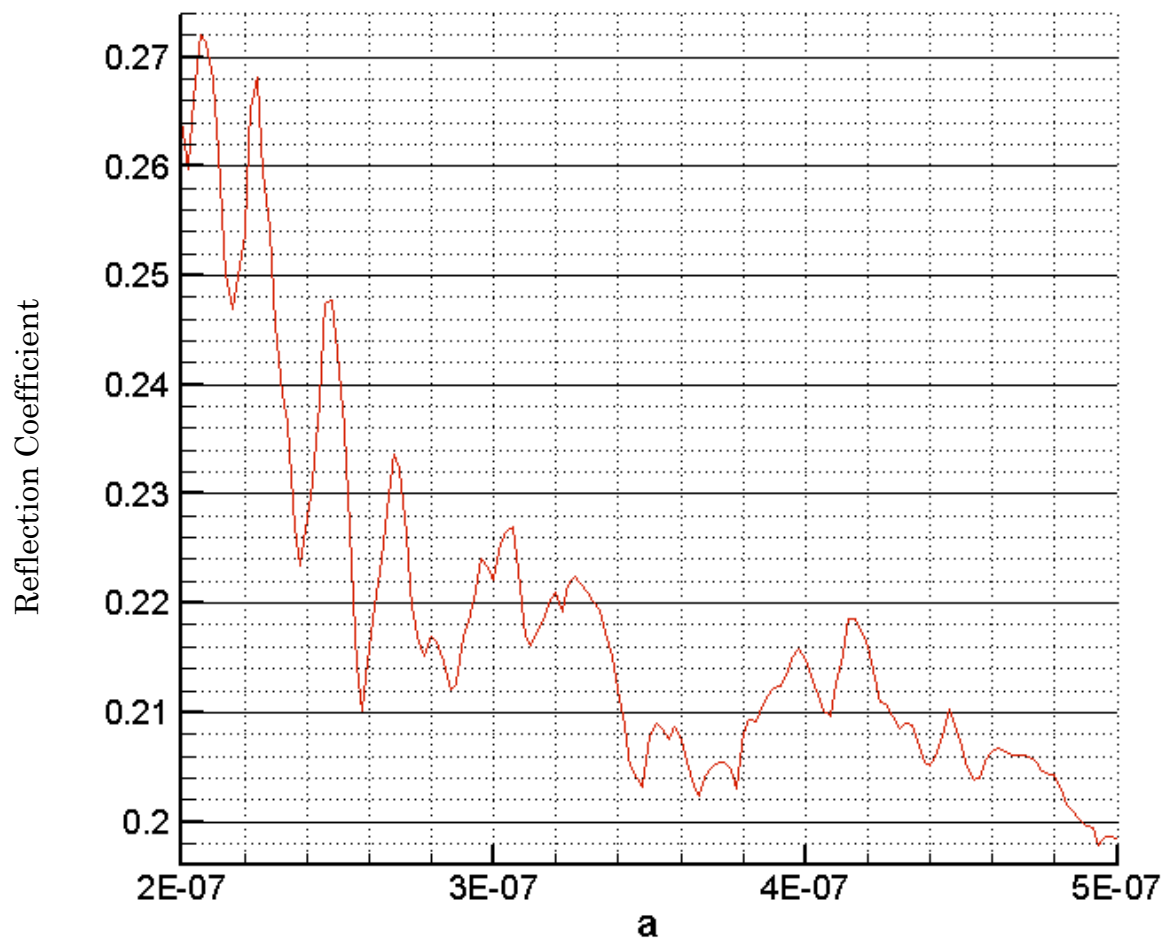


Figure 9

Radius of Sphere /m